Interpretation of Mixed-Valence Compound Optical Spectra Near the Class II/III Border: Dinitrobiphenyl and Dinitrophenanthrene Radical Anions

Stephen F. Nelsen,*,† Kevin P. Schultz,† and João P. Telo*,‡

Department of Chemistry, University of Wisconsin, 1101 University Avenue, Madison, Wisconsin 53706-1396, and Centro de Química Estrutural, Instituto Superior Técnico, Av. Rovisco Pais, 1049-001 Lisboa, Portugal

Received: August 26, 2008; Revised Manuscript Received: October 10, 2008

The optical spectra of 4,4′-dinitrobiphenyl and other similar 9-bond bridged radical anions show that these mixed-valence compounds are predominantly charge-localized in the high λ_S solvent MeCN, charge-delocalized in the low λ_S solvent HMPA, and show intermediate behavior in DMF. Hush analysis of the localized charge-transfer band in MeCN allowed the calculation of the electronic coupling between nitro groups (H_{ab}). H_{ab} changes with bridge structure, depending mainly on the twist angle between the two aromatic rings: H_{ab} is higher for the planar 9,9-dimethyl-2,7-dinitrofluorene radical anion (1100 cm^{-1}) and about one-half of this value for the more twisted 2,2′-dimethyl-4,4′-dinitrobiphenyl radical anion (540 cm^{-1}). The reorganization energy λ decreases as H_{ab} increases. We suggest that this is due to a decrease of the internal reorganization energy λ_v as the Class II/Class III borderline is approached, and that λ_v should be zero at the borderline. Subtracting from the experimental spectra the fraction corresponding to the delocalized part (taken as the spectrum in HMPA or THF), we get localized charge-transfer bands that show a significant cutoff effect at the low energy side, as predicted by classical Marcus−Hush theory.

Introduction

Symmetrical dinitroaromatic radical anions were among the first organic mixed-valence compounds for which intramolecular electron-transfer reactions were studied by EPR spectroscopy.[1] However, these systems were not discussed as mixed-valence (MV) systems because this concept was only developed in the later 1960s for transition-metal coordination compounds by Robin and Day[2] and Hush.[3] MV compounds have two charge-bearing units (CBUs) M symmetrically connected by a bridge B and have an odd overall charge, so that the two M units may be at different redox levels. According to the Robin and Day classification,[2] Class II (localized) mixed-valence compounds are described as two charge-localized structures in equilibrium, $M^0-B-M^{-1} \leftrightarrows M^{-1}-B-M^0$. Each of these charge-localized structures corresponds to a minimum in the adiabatic potential surface of the ground state (see Figure 1). Class III (delocalized) mixed-valence compounds have instantaneously the same fractional charge at the two M units and, in the case of having a single negative overall charge, can be described as $M^{-1/2}-B-M^{-1/2}$, although significant charge is also present on the bridge of Class III compounds. In the Marcus−Hush two-state model,[4] the shape of the adiabatic potential surfaces depends only on two parameters: the reorganization energy λ, and the electronic coupling between the charge-bearing units H_{ab}. The Class II double-minimum ground-state surface occur for systems with $\lambda > 2H_{ab}$. At $\lambda = 2H_{ab}$, the two minima merge into a single one at the II/III borderline, and for $\lambda < 2H_{ab}$ the system is charge-delocalized (Class III, Figure 1).

MV systems close to the Class II/III transition have attracted considerable attention in the recent past.[5,6] We reported previously on dinitroaromatic radical anions close enough to the Class III/Class II borderline that changing the solvent induces the change from a delocalized mixed-valence compound to a localized one.[7,8] The optical spectra of the 11-bond bridged ($n = 11$) **1**$^-$ and **2**$^-$ (see Chart 1) show the low energy optical band with narrow bandwidths and partially resolved vibrational structure that are typical for Class III dinitroaromic radical anions[9,10] in THF and HMPA. However, in DMF, DMSO, and

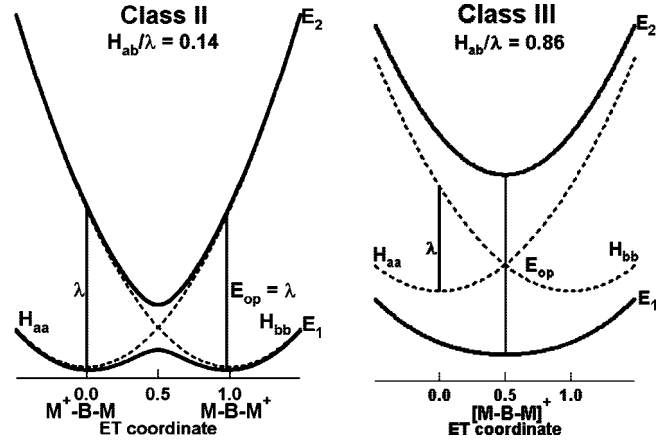

Figure 1. Marcus−Hush diagrams for localized (Class II) and delocalized (Class III) mixed-valence compounds.

CHART 1: Some Previously Studied Dinitroaromatics

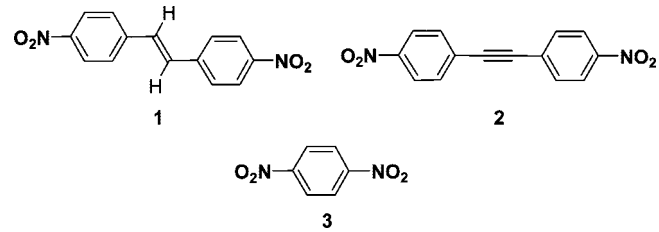

* Corresponding authors. E-mail: nelsen@chem.wisc.edu (S.F.N.); jptelo@ist.utl.pt (J.P.T.).
† University of Wisconsin.
‡ Instituto Superior Técnico.

10.1021/jp807602k CCC: $40.75
Published on Web 11/18/2008

CHART 2: Structures of the Dinitroaromatics Discussed Here

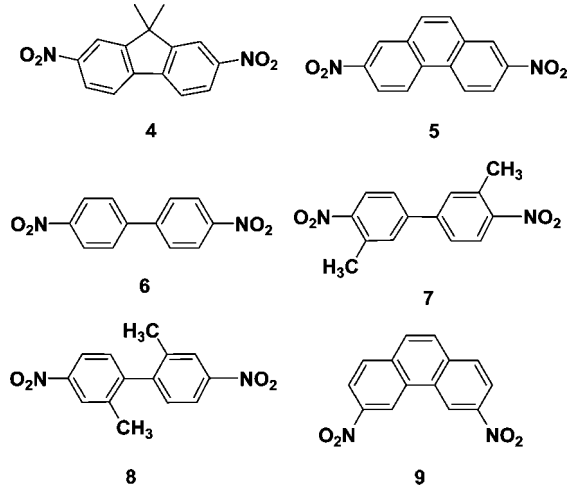

MeCN, it shows the broad and featureless Gaussian-shaped band typical of Class II localized species, with values of λ, taken as the energy maximum of the charge-transfer band, increasing in that order.[8] This change of behavior occurs because the reorganization energy is largely dominated by the solvent reorganization energy λ_S, with total λ exceeding $2H_{ab}$ in the high λ_S solvents DMF, DMSO, and MeCN, but being smaller than $2H_{ab}$ in solvents that interact less strongly with the reduced nitro group.

In contrast to **1**$^-$ and **2**$^-$, the radical anion of **3** and those of several other dinitroaromatic radical anions having the Kekule substitution pattern that cause large electronic couplings through the bridge are delocalized (Class III) in DMF.[10] The 5-bond-bridged **3**$^-$ produces the delocalized spectrum in all aprotic solvents studied. A smaller distance between charge bearing units decreases the reorganization energy (through its solvent reorganization, λ_S, term) and increases the electronic coupling H_{ab}, maintaining a $\lambda/2H_{ab}$ ratio lower than one even in solvents that produce higher λ_S values. However, when **3**$^-$ is prepared in alcohols, hydrogen bonding to the solvent causes charge localization, as shown by the alternating line broadening effects induced by the intramolecular electron-transfer reaction in their EPR spectra.[11]

We consider here the optical spectra and the reorganization energies and electronic couplings that they reveal for the radical anions of some additional dinitroaromatic compounds that have $n = 9$ (**4**−**8**, see Chart 2), as well as the related 3,6-dinitrophenanthrene (**9**). Their radical anions also mostly lie near enough to the Class II/III borderline that they become delocalized in low λ_s solvents. **4** and **5** have the 2,2′ biphenyl carbons bridged by substituents that prevent twisting about the central C−C bond, while **6** and **7** will be twisted somewhat, and **8** has double *ortho*-methyl substitution that will force considerably more twisting. The larger π system of 2,7-dinitrophenanthrene **5**$^-$ than the biphenyl derivatives **4**$^-$ and **6**$^-$−**8**$^-$ also influences the electronic coupling. 3,6-Dinitrophenanthrene (**9**) formally has an $n = 7$ bond shortest pathway, but because the central bond of its biphenyl system is meta to both nitro groups, its substitution pattern is non-Kekule with respect to this shorter bridge, and the 11-bond *cis*-stilbene pathway is expected to predominate, so the electronic coupling for **6**$^-$ should be more like that of the *trans*-dinitrostilbene **1**$^-$ than that of an $n = 7$ compound.

TABLE 1: Class II Band and Hush-type Analysis of Dinitroaromatic Radical Anions in MeCN[a]

cmpd	n	E_{op}	ε_{max}	$\Delta\bar{\nu}_{1/2}$[b]	d_{12}[c]	d_{ab}[c]	H_{ab}[d]	$2H_{ab}/\lambda$	θ[e]
4$^-$	9	∼9700	5790	∼5700	9.07	9.37	∼1100	0.23	0
5$^-$	9	9880	3580	6220	9.36	9.55	900	0.20	0
6$^-$	9	10 260	3720	6150	9.30	9.49	930	0.18	32
7$^-$	9	10 300	2240	5560	9.04	9.15	710	0.14	31
8$^-$	9	12 800	910	6720	9.37	9.41	540	0.08	55
9$^-$	11	9730			10.34	10.39	445	0.09	
1$^-$	11	9680			11.22	11.31	545	0.11	

[a] Units: cm^{-1} (energies); M^{-1} cm^{-1} (ε); Å (distances). [b] Band width at half-height measured from spectra with the dianion subtracted. [c] Calculated from the dipole moment calculated by AM1 as previously described.[14] Charge localization was achieved by using the COSMO calculation[15] option in program VAMP.[16] [d] Estimated by Hush's method, but including a refractive index correction. [e] Twist angle around the central bond of the biphenyl system, calculated by AM1.

Experimental Section

9,9-Dimethyl-2,7-dinitrofluorene **4** was purchased from Aldrich. Substituted biphenyls **6**, **7**, and **8** were prepared by Ullmann coupling of the appropriate iodonitrobenzenes. Dinitrophenanthrenes **5** and **9** were prepared by the method of Bacon and Lindsay.[12]

2,7-Dinitrophenanthrene (5). mp >300 °C (toluene); ^{1}H NMR (300 MHz, DMSO-d_6) δ 8.31 (s, 2H), 8.48 (d, 2H, J = 8.6 Hz), 9.07 (s, 2H), 9.17 (d, 2H, J = 8.6 Hz); UV (DMF) 347 nm (log ε = 4.26); EPR (radical anion, MeCN) a_{2N} = 3.15 G, a_{2H} = 1.94 G, a_{2H} = 0.66 G, a_{2H} = 0.22 G, a_{2H} = 0.11 G.

3,6-Dinitrophenanthrene (9). mp 285−287 °C (toluene, lit.[12] 282−283 °C); ^{1}H NMR (300 MHz, DMSO-d_6) δ 8.29 (s, 2H), 8.37 (d, 2H, J = 8.9 Hz), 8.52 (dd, 2H, J = 8.9, 1.6 Hz), 9.80 (d, 2H, J = 1.6 Hz); UV (DMF) 327 nm (log ε = 4.17); EPR (radical anion, MeCN) a_{2N} = 3.14 G, a_{2H} = 1.91 G, a_{2H} = 1.11 G, a_{2H} = 0.69 G, $a_{2H} \approx 0$ G.

The radical anions were prepared in vacuum-sealed glass cells equipped with an ESR tube and a quartz optical cell. Reduction was achieved by contact with 0.2% Na−Hg amalgam. The nitro compound, an excess of commercial cryptand[2.2.2], and the Na−Hg amalgam were introduced in different chambers of the cell under nitrogen. The cryptand was degassed by melting under high vacuum before addition of the solvent. The concentration of the samples was determined spectrophotometrically before reduction. UV/vis/NIR spectra were recorded at room temperature with a Shimadzu 3101 PC spectrometer at several stages of reduction, so that the maximum radical anion oxidation level spectrum could be selected. A small proportion of dianion formed by electron-transfer disproportionation is also present in the samples and was subtracted from the optical spectra before estimating the charge-transfer band parameters in Table 1.

Results

The optical spectra of **4**$^{\bullet-}$ in THF ($\bar{\nu}_{max}$ = 6940 cm^{-1}, $\varepsilon_{max} \approx$ 47 000) and HMPA ($\bar{\nu}_{max}$ = 6910 cm^{-1}, $\varepsilon_{max} \approx$ 23 000), see Figure 2, have quite similar band maxima and show partially resolved vibrational fine structure, demonstrating that **4**$^{\bullet-}$ is charge delocalized (Class III) in these solvents. The spectrum obtained in HMPA was only about half as intense. The accuracy of the ε values is not entirely clear, because the samples are prepared by sodium amalgum reductions in sealed tubes and only the amounts of starting neutral compound are known accurately; the ε values were calculated assuming a 100% yield

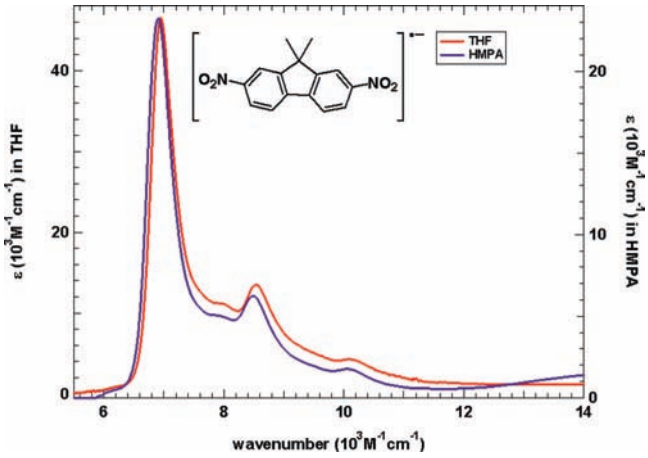

Figure 2. Spectra of 9,9-dimethyl-2,7-dinitrofluorene radical anion **4**$^{\bullet-}$ in THF and HMPA, plotted at the same height on different axes to allow comparison of the band shape.

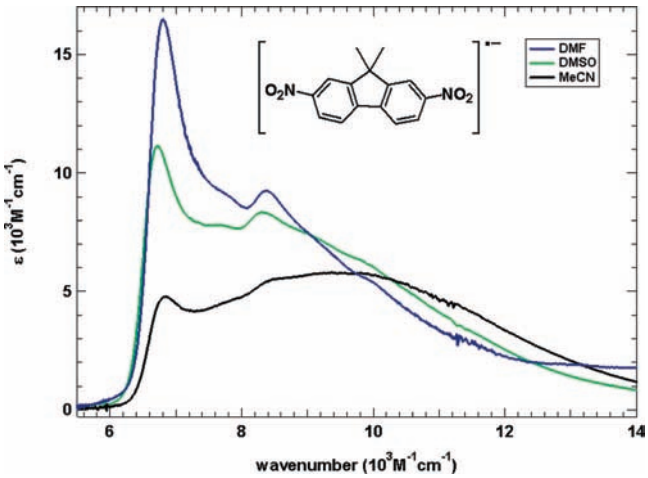

Figure 3. Spectra of 9,9-dimethyl-2,7-dinitrofluorene radical anion **4**$^{\bullet-}$ in DMF, DMSO, and MeCN.

of radical anion. The higher energy "fine structure" is seen to be slightly less intense relative to the maximum in the HMPA spectrum.

The spectra of **4**$^{\bullet-}$ in DMF, DMSO, and MeCN, Figure 3, show increasingly larger amounts of the higher energy broad absorption that is characteristic of the MV charge-transfer band of charge localized (Class II) dinitroaromatic radical anions in that order. The spectra in these solvents are assigned as a weighted sum of two components: the vibration progression with narrow bandwidth corresponding to the delocalized (Class III) material and the broad and Gaussian-shaped band typical of localized (Class II) compounds, which does not show vibrational features because of the steep slope of the excited-state energy surface vertical from the minimum.[13]

The optical spectra of **5**$^{-}$ in three solvents are compared in Figure 4, those of the biphenyls **6**$^{-}$, **7**$^{-}$, and **8**$^{-}$ in various solvents in Figures 5 to 7, and those of 3,6-dinitrophenanthrene **9**$^{-}$ in Figure 8.

The least overlap between the Class II and Class III spectra occurs for the highest λ_s solvent studied, acetonitrile, and the details of a Hush-type analysis of the spectra in acetonitrile are shown in Table 1. The increase in λ_v that is expected when the central bond of the biphenyl system has greater twist is reflected in the E_{op} values that are observed for **6**$^{-}$−**8**$^{-}$ as compared to the untwisted **4**$^{-}$ and **5**$^{-}$. The H_{ab} values for **4**$^{-}$ and **6**$^{-}$ are close to the cos θ relationship expected, and that obtained for **8**$^{-}$ is

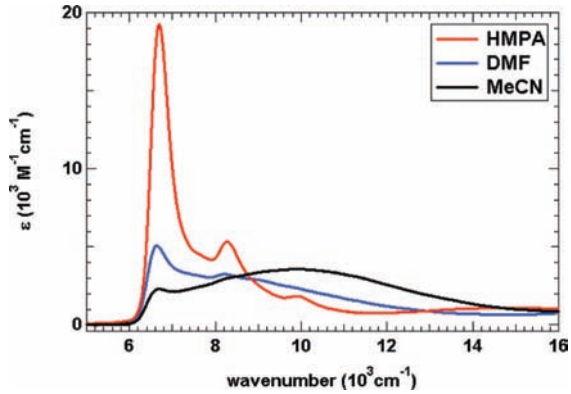

Figure 4. Optical spectra of 2,7-dinitrophenanthrene radical anion (**5**$^{-}$) in three solvents.

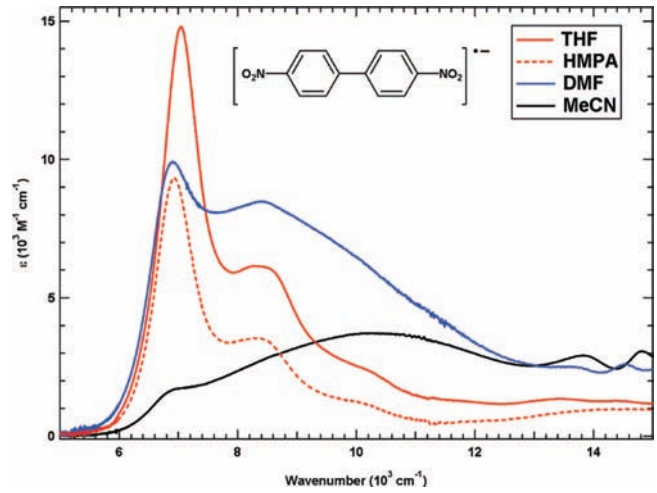

Figure 5. Optical spectra of 4,4′-dinitrobiphenyl radical anion (**6**$^{-}$) in four solvents.

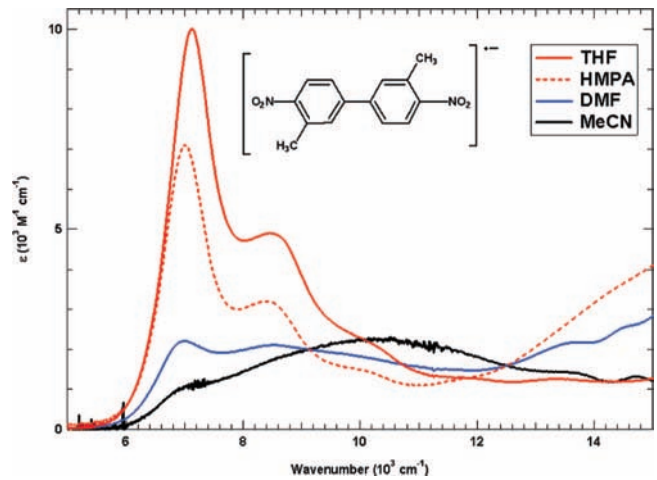

Figure 6. Optical spectra of 3,3′-dimethyl-4,4′-dinitrobiphenyl radical anion (**7**$^{-}$) in four solvents.

86% as large as predicted from the AM1 θ value. The 3,3′-dimethyl substitution of **7**$^{-}$ is not calculated to either affect the θ or twist the nitro groups out of overlap, but it is calculated to change the electron distribution and hence lower the dipole moment and hence d_{ab}, resulting in a drop of about 24% in the optical H_{ab} value relative to the unmethylated compound **4**$^{-}$. The $2H_{ab}/\lambda$ values, which as discussed below are the criterion we use for approach to the II/III borderline (which occurs at $2H_{ab}/\lambda = 1$), range down from 0.23 for **4**$^{-}$, so all of these compounds appear to be strongly trapped in acetonitrile.

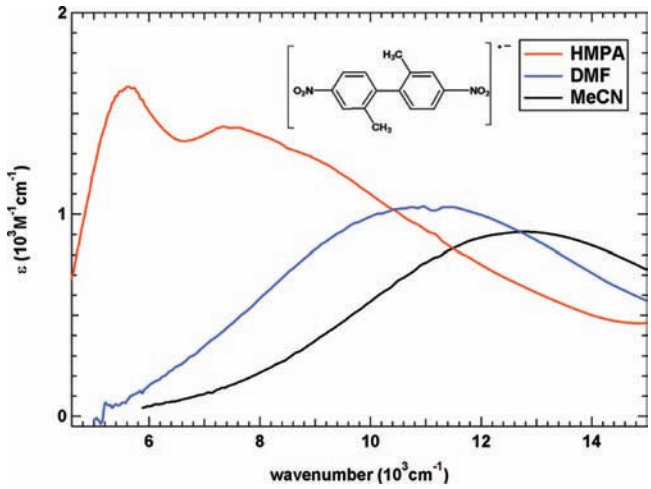

Figure 7. Optical spectra of 2,2′-dimethyl-4,4′-dinitrobiphenyl radical anion (**8**$^-$) in three solvents.

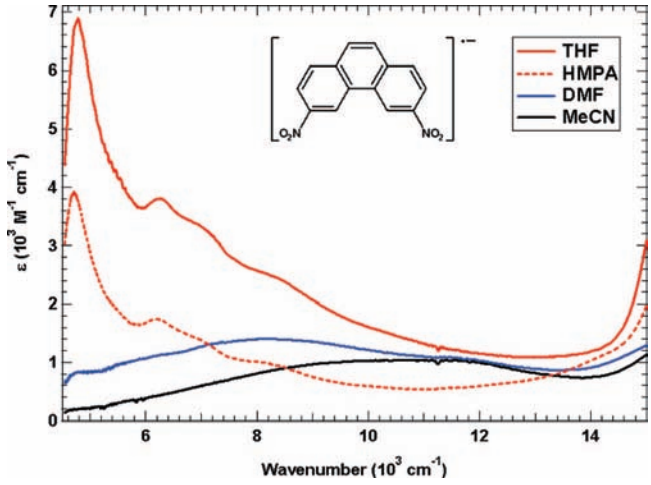

Figure 8. Optical spectra of 3,6-dinitrophenanthrene radical anion (**9**$^-$) in four solvents.

However, this ratio seems low for compounds such as **4**$^-$−**7**$^-$ that are close enough to the Class II/Class III border that changing the solvent to HMPA causes delocalization. This suggests that H_{ab} is being underestimated by the Hush equation in this region. In fact, although the Hush two-state model predicts the intramolecular electron-transfer rate constant surprisingly well for the strongly trapped 2,7-dinitronaphthalene radical anion,[17] for other dinitro radical anions close to the Class II/III borderline, like 4,4′-dinitrotolane **1**$^-$ and 4,4′-dinitrostilbene **2**$^-$, H_{ab} is significantly underestimated by the Hush equation.[8] The twist in **8**$^-$ makes it slightly more strongly trapped than either of the $n = 11$ compounds discussed here.

As discussed in detail previously,[8] E_{op} for Class III dinitroaromatic radical anions can be rather accurately calculated using the "neutral in anion geometry" (NAG) method in which the odd electron-containing MO is artificially emptied by calculating the neutral compound at the geometry of the radical anion. Perhaps surprisingly, having the same number of electrons (zero) in both MOs causes the energy gap to be as good of an approximation to the observed transition energy as Koopmans' theorem provides for the filled MO to SOMO transitions that are usually the lowest energy transition for delocalized radical cations.[18] These calculations, applied for the compounds discussed here, are shown in Table 2. By far the poorest agreement is shown by the twisted biphenyl **8**$^-$, which along with the smaller than expected from the calculated θ value (Table 1)

TABLE 2: Band Maxima for Low Energy Band of the Delocalized Spectra in HMPA and NAG Calculations

cmpd	n	E_{op} (cm^{-1}) exp.	E_{op} (cm^{-1}) calcd. NAG	(calc. − exp.) (cm^{-1})
4$^-$	9	6910	6780	−130
5$^-$	9	6700	6570	−130
6$^-$	9	7040	6740	−300
7$^-$	9	7010	6925	−85
8$^-$	9	5600	4640	−960
9$^-$	11	4710	5000	+290

suggests to us that the AM1 calculation probably underestimates the effective amount of twist in both the localized and the delocalized radical anions of this compound. Koopmans-based calculations and experimental spectra for the phenanthrene radical anions **5**$^-$ and **9**$^-$ are shown in the Supporting Information.

Discussion

Interpretation of Band Maximum Near the II/III Border. Figure 9 shows a diagram indicating how one might traditionally consider a plot of the energy and interpretation of E_{op} for localized and delocalized MV dinitroaromatic radical anions. It has been assumed that a single two-state model can be used for delocalized MV compounds, which makes $E_{op} = 2H_{ab}$, and that $E_{op} = \lambda$ for localized ones, and because λ_s predominantly is caused by electrostatic interaction of the solvent with the large dipole moment (μ) of a localized compound, that dielectric continuum theory suffices to describe the size of λ_s so that E_{op} will decrease linearly as the solvent parameter $\gamma = 1/n^2 - 1/\varepsilon_s$ drops, as long as localized material remains lower in energy than delocalized material. When the delocalized material becomes more stable, one would see the spectrum of delocalized material appear, for which E_{op} would be constant unless the structure changed enough to alter H_{ab}. However, E_{op} for Class III MV species proves not to be constant with solvent[19] and depends upon how close to the II/III border the compound lies, although the variation is always smaller than that for Class II compounds. It is also now clear experimentally that dielectric continuum theory does not properly describe how E_{op} changes with solvent for localized compounds, for example, because of the very different behavior of Class II MV radical cations and radical anions. These experimental observations suggest that Figure 9 does not provide a useful model for considering what happens near the II/III border, as discussed below.

According to the two-state model, the transition energy of the lowest energy band of delocalized Class III compounds has been assumed to equal $2H_{ab}$, as we believe was first pointed out explicitly by Creutz in 1983,[20] and has been extensively applied by many workers to the lowest energy intense absorption band for Class III MV systems since the four papers we have found that were published making this assumption in 1990.[21−24] However, there is a problem with this interpretation, which has been pointed out more recently. As is well-known, the transition observed is between MOs of different symmetry, so it is definitely not between the upper and lower levels of a single two-state diagram that the $E_{op} = 2H_{ab}$ equation assumes (MOs of different symmetry do not split each other). The two-state model does not apply unaltered to the optical spectra of Class III compounds, because there are two diabatic M combination orbitals, which for Class III compounds are the symmetric and antisymmetric combinations of the individual M group orbitals (the nitro group in this case) relative to a plane bisecting the molecule. They interact separately with the symmetric and antisymmetric bridge diabatic orbitals. Zink and Nelsen have

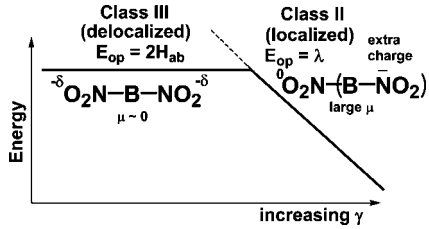

Figure 9. Diagram for energies and interpretation of E_{op} using the traditional single two-state model and proportionality of λ_s to γ.

pointed out that the simplest analysis that could produce meaningful couplings, which they called the Neighboring Orbital model,[10,25−27] demonstrates that E_{op} for the lowest energy Class III band is determined by at least two electronic couplings and three diabatic energy levels. The diabatic energy levels clearly are affected by solvent, as well as by aromatic substituent effects. This is consistent with the observed dependence of E_{op} for Class III compounds upon solvent. The question is not whether the energy surfaces should look like they do at the right side of Figure 1 for a Class III compound (they do), but whether the lowest energy transition observed for such a compound corresponds to what is labeled as E_{op} (it is not).

In considering $E_{op} = \lambda$ for Class II compounds, it has traditionally been implicitly assumed that λ_v is constant, so that all of the variation of E_{op} can be attributed to changes in λ_s. We note that, although this is a good assumption for strongly trapped Class II MV compounds, it cannot be true near the II/III border because increasing H_{ab} causes mixing of the wave functions for the two CBUs that eventually results in their geometries becoming the same and λ_v disappearing entirely, at the border. As we believe was first pointed out explicitly by Sutin, the solutions for the ground-state and excited-state adiabatic surfaces, E_1 and E_2, respectively, are:

$$E_1 = 0.5[\lambda(2X^2 - 2X + 1) + \Delta G^\circ] - 0.5[\{\lambda(2X - 1) - \Delta G^\circ\}^2 + 4(H_{ab})^2]^{1/2} \quad (1)$$

$$E_2 = 0.5[\lambda(2X^2 - 2X + 1) + \Delta G^\circ] - 0.5[\{\lambda(2X - 1) - \Delta G^\circ\}^2 + 4(H_{ab})^2]^{1/2} \quad (2)$$

X is Marcus's normalized electron-transfer coordinate, for which the minima of the diabatic parabolas occur at $X = 0$ and 1. Because the CBUs for the cases under consideration are the same, $\Delta G^\circ = 0$. As H_{ab} increases, mixing of the wave functions for $M^{(-)}$ and M^0 occurs, which moves the minima on the adiabatic ground-state surface, E_1, toward $X = 0.5$, and causes the geometries of the CBUs to become increasingly similar to each other. The minimum on E_1 closest to $X = 0$, X_{min}, is given by eq 3:

$$X_{min} = 0.5[1 - (1 - 4H_{ab}^2/\lambda^2)^{1/2}] \quad (3)$$

and the minimum for the one closest to $X = 1$ is $(1 - X_{min})$. The ratio of the ET distance on E_1 to that on the diabatic surfaces is $(1 - 2X_{min})$. We suggest that λ_v as a function of H_{ab} is proportional to $(1 - 2X_{min})$, which is plotted in Figure 10 against $2H_{ab}/\lambda$. This plot shows that λ_v indeed changes slowly initially: for the first 40% of the way from $H_{ab} = 0$ to $H_{ab} = \lambda/2$ (between $2H_{ab}/\lambda = 0$ and 0.4), $(1 - 2X_{min})$ only decreases from 1.00 to 0.92. However, approach of the adiabatic minima becomes far more rapid as $2H_{ab}$ approaches λ near the Class II/III borderline. For the last 10%, $2H_{ab}/\lambda = 0.9-1.0$, $(1 - 2X_{min})$ decreases from 0.436 to 0, approaching the Class II/III borderline with a limiting slope of infinity. Figure 10 suggests that as the II/III border is approached, the principal factor affecting E_{op} will be the drop of λ_v, not a change in λ_s.

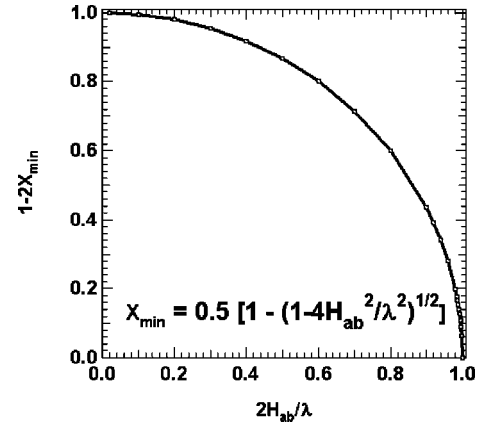

Figure 10. Plot of $(1 - 2X_{min})$ versus $2H_{ab}/\lambda$.

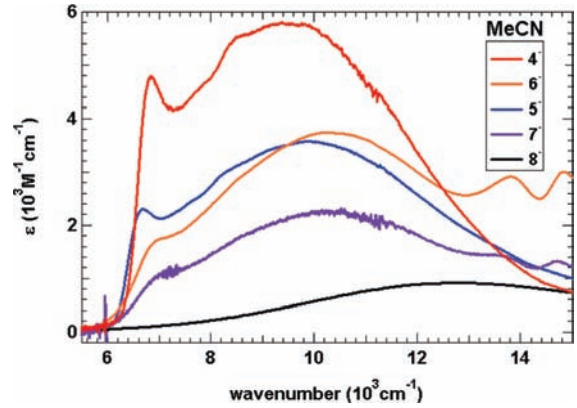

Figure 11. Optical spectra of $\mathbf{4}^{-}$−$\mathbf{8}^{-}$ in MeCN.

The low dipole moment Class III species and high dipole moment Class II species will be solvated quite differently, especially considering the relatively unhindered and high charge density nitro groups in the dinitroaromatic radical anions considered here, for which specific solvation effects are clearly important. We do not think that it is easy to predict how the relative amounts of the localized and delocalized material should change as solvent is changed, but suggest that because the two have significantly different spectra for these compounds,[28] their spectra, compared in acetonitrile in Figure 11, demonstrate that increasingly small but detectable amounts of the delocalized species are present even in the high λ_s solvent acetonitrile for $\mathbf{4}^{-}$−$\mathbf{7}^{-}$, and that delocalized material becomes undetectable only for $\mathbf{8}^{-}$. Thus, experimentally, instead of the rather sharp break between the presence of localized and delocalized material that is suggested by Figure 9 (for which delocalized material would presumably only be seen for a range of γ that corresponded to a λ_s change of about 2.8 kcal/mol (980 cm^{-1}, corresponding to a 2 orders of magnitude change in concentration of delocalized material)), experimentally the range in E_{op} for the localized material over which delocalized material is observed is far greater. The spectra of $\mathbf{4}^{-}$−$\mathbf{8}^{-}$ in HMPA are shown in Figure 12, where it is seen that delocalized material predominates for all but the very twisted $\mathbf{8}^{-}$, which has an unusually weak, broad, and low energy absorption in a region that can only be reasonably attributed to delocalized material. Unfortunately, we do not have a good way of estimating what ε is for the delocalized material.

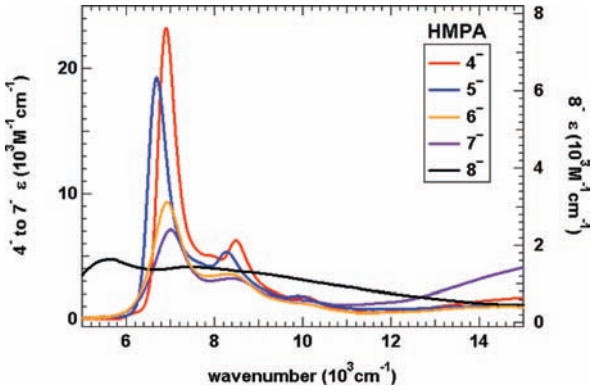

Figure 12. Optical spectra of **4**$^-$−**8**$^-$ in HMPA.

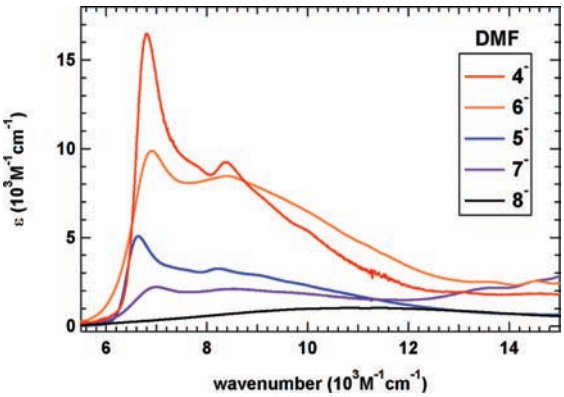

Figure 13. Optical spectra of **4**$^-$−**8**$^-$ in DMF.

The ratios of ε_{max} in THF to that in HMPA we obtained are 2.00 for **4**$^-$, 1.59 for **6**$^-$, 1.43 for **7**$^-$, and 1.76 for **9**$^-$. This represents much greater sensitivity of ε_{max} to solvent than we would have expected. Although extinction coefficients are often assumed to depend upon the refractive index of the solvent, corrections first applied by the Kodak group for interpreting electron-transfer processes,[29] we have not seen an expression that would cause such a large change. Unfortunately, solubility problems prevented obtaining spectra for the other compounds in THF.

Spectra of **4**$^-$−**8**$^-$ in the intermediate λ_s solvent DMF are shown in Figure 13. Substantially more intense absorption for the delocalized material relative to localized material is seen for each compound than in acetonitrile.

Band Shape for Localized Material Near the II/III Border. We next examine whether subtraction of the spectra of the narrower and more intense delocalized component of the spectrum might give clearer spectra of the localized (Class II) components. The most favorable case to consider is **4**$^-$, which is presumably closest to the borderline because it has the largest amount of delocalized feature present in the highest λ_s solvent, MeCN. We subtracted various percentages of the spectra in both HMPA and THF, moved arbitrarily on the wavenumber axis to make the sharper components overlap, to obtain what appears to us to be elimination of the Class III component of the spectrum. It is necessary to use twice as large a percentage of the HMPA spectrum as the THF spectrum, because the ε_{max} obtained was about twice as large for the THF spectrum (see Figure 2). The Supporting Information compares the experimental spectra with those obtained after subtraction of both the HMPA and the THF spectra in MeCN, DMSO, and DMF, and shows the sizes of the shifts of the "delocalized" spectra necessary to achieve overlap (74−225 cm^{-1}). Figure 14

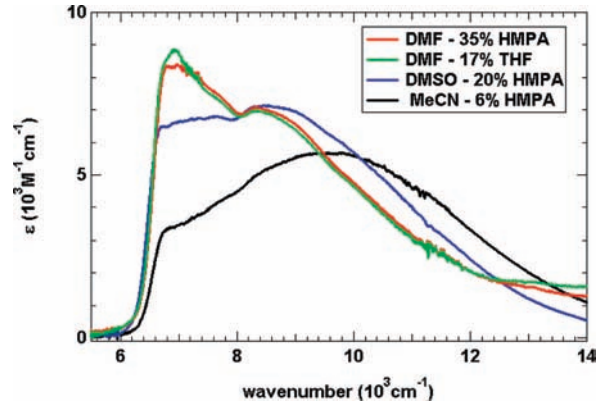

Figure 14. Comparison of the Class II region spectra of **4**$^-$ obtained by subtraction of scaled HMPA or THF spectra.

compares the band shapes obtained after subtraction for three of the solvents, MeCN, DMSO, and DMF. Both the HMPA and the THF difference spectra are only shown for DMF, which had the largest difference, because the amounts subtracted were the largest. All spectra show a substantial "cutoff" appearance, as one of us suggested should occur near the Class II/III borderline using a classical Hush analysis.[30] It will be noted that the second larger vibrational feature near 8200 cm^{-1} is not subtracted exactly correctly in any of the solvents, presumably because the band widths are different in different solvents. Not surprisingly, the anomalous absorption changes in this region are largest in DMF, where the largest subtraction was done. The cutoff is clearly nearest the low energy edge of the Class II band in MeCN, closer to the maximum in DMSO, and might even still be on the rising portion of the Class II spectrum in DMF. The maximum of the residual, which is hoped to be the absorption for localized (Class II) material, is about 9700 cm^{-1} in MeCN, about 8500 cm^{-1} (1200 cm^{-1} lower) in DMSO, and about 6900 cm^{-1} (2800 cm^{-1} lower) in DMF. The Supporting Information shows similar subtraction spectra for **5**$^-$ in MeCN and DMF.

According to the two-state model, the cutoff should occur when the energy equals $2H_{ab}$. This would lead to $H_{ab} = 3300$ cm^{-1} for **4**$^-$ in MeCN. This value is substantially bigger than the 1100 cm^{-1} value calculated by the Hush equation from the band parameters (Table 1), but seems much more reasonable for a compound so close to the Class II/Class III borderline. As stated before, the Hush equation gives unreasonably low values for H_{ab} in mixed-valence Class II compounds close to the borderline. Applying the $H_{ab} = 3300$ cm^{-1} value to the energy barrier equation, $\Delta G^* = \lambda/4 - H_{ab} + (H_{ab})^2/\lambda$, yields $\Delta G^* =$ 248 cm^{-1} in MeCN and $\Delta G^* = 106$ cm^{-1} in DMSO. The value of the energy barrier for **4**$^-$ is just above RT in MeCN ($RT =$ 203 cm^{-1} at 20 °C) and well below it in DMSO, which is consistent with the fact that **4**$^-$ is close to the Class II/Class III border. However, the ratio of the ET distance on the lower energy surface to that on the diabatic surfaces, $1 - 2X_{min}$, is 0.73 in MeCN and 0.63 in DMSO, so the two adiabatic minima obtained from the Class II features of its spectrum are still estimated to be far from merging in these two solvents. Nevertheless, the Class III features that were subtracted in Figure 14 are also observed, implying that the Class II and Class III species are close in energy. Because they will be very differently solvated, we do not think that dielectric continuum theory is suitable to try to estimate what their energy difference should be.

Conclusions

The optical spectra of the radical anions from dinitrobiphenyls **6**, **7**, and **8** and other similar 9-bond bridged systems, like the 9,9-dimethyl-2,7-dinitrofluorene **4** and 2,7-dinitrophenanthrene **5**, show that these mixed-valence compounds are charge-localized in the high λ_S solvent MeCN, charge-delocalized in the low λ_S solvents HMPA and THF, and show intermediate behavior in DMF, where both kinds of spectra are observed. Calculation of the electronic coupling between nitro groups (H_{ab}) using the Hush analysis of the localized charge-transfer band in MeCN shows that H_{ab} changes with bridge structure, depending mainly on the twist angle between the two aromatic rings. H_{ab} is higher in these 9-bond bridged systems than in the previously studied 11-bond bridge ones such as 4,4′-dinitrotolane and 4,4′-dinitrostilbene radical anions, confirming the theoretical prediction that the electronic coupling decreases with the distance between charge-bearing units. However, the fact that 3,6-dinitrophenanthrene radical anion, which has an 11-bond conjugation pathway between nitro groups, shows a smaller H_{ab} than does its 2,7-dinitrophenanthrene isomer, which is 9-bond bridged but with a longer d_{NN} distance, shows that the "distance" should be carefully evaluated in terms of bonds between charge bearing units.

The reorganization energy, λ, taken as the maximum of the localized band in MeCN, is lower for the systems closer to the Class II/Class III borderline. Because the distance between charge bearing units does not change much in the compounds studied, we suggest that λ decreases due to a decrease in the internal reorganization energy (λ_v), which will disappear entirely at the Class II/Class III borderline due to the averaging of the geometries of the two CBUs. Subtracting from the experimental spectra of $\mathbf{4}^-$ in each solvent a weighted amount of the delocalized spectra in HMPA or THF yielded what we suggest is the localized component of each spectrum. The charge-transfer bands thus obtained show a clear cutoff effect at the low energy side, as predicted by classical Hush theory.

Acknowledgment. We thank the National Science Foundation for support of this work under CHE-0647719 (S.F.N.) and Fundação Para a Ciência e Tecnologia through its Centro de Química Estrutural (J.P.T.).

Supporting Information Available: Comparison of the observed spectrum of $\mathbf{4}^-$ with those having weighted and shifted THF and HMPA spectra subtracted in MeCN, DMSO, and DMF, and similar information for $\mathbf{5}^-$ with HMPA spectra subtracted in MeCN and DMF. Comparison of observed and Koopmans-based calculated spectra for $\mathbf{5}^-$ and $\mathbf{9}^-$. This material is available free of charge via the Internet at http://pubs.acs.org.

References and Notes

(1) (a) Maki, A. H.; Geske, D. H. *J. Chem. Phys.* **1960**, *33*, 825. (b) Maki, A. H.; Geske, D. H. *J. Am. Chem. Soc.* **1961**, *83*, 1852. (c) Freed, J. H.; Rieger, P. H.; Fraenkel, G. K. *J. Chem. Phys.* **1962**, *37*, 1881. (d) Freed, J. H.; Fraenkel, G. K. *J. Chem. Phys.* **1963**, *39*, 326. (e) Rieger, P. H.; Fraenkel, G. K. *J. Chem. Phys.* **1963**, *39*, 609. (f) Harriman, J. E.; Maki, A. H. *J. Chem. Phys.* **1963**, *39*, 778. (g) Freed, J. H.; Fraenkel, G. K. *J. Chem. Phys.* **1964**, *41*, 699. (h) Geske, D. H.; Ragle, J. L.; Bambenek, M. A.; Balch, A. L. *J. Am. Chem. Soc.* **1964**, *86*, 987. (i) Blandamer, M. J.; Gough, T. E.; Gross, J. M.; Symons, M. C. R. *J. Chem. Soc.* **1964**, 536.

(2) Robin, M.; Day, P. *Adv. Inorg. Radiochem.* **1967**, *10*, 247.

(3) (a) Hush, N. S. *Prog. Inorg. Chem.* **1967**, *8*, 391–444. (b) Hush, N. S. *Electrochim. Acta* **1968**, *13*, 1005.

(4) (a) Marcus, R. A. *J. Chem. Phys.* **1956**, *24*, 966–978. (b) Marcus, R. A.; Sutin, N. *Biochim. Biophys. Acta* **1985**, *811*, 265. (c) Hush, N. S. *Prog. Inorg. Chem.* **1967**, *8*, 391–444. (d) Hush, N. S. *Coord. Chem. Rev.* **1985**, *64*, 135.

(5) (a) Nelsen, S. F. *Chem.-Eur. J.* **2000**, *6*, 581–588. (b) Demadis, K. D.; Hartshorn, C. M.; Meyer, T. J. *Chem. Rev.* **2001**, *101*, 2655. (c) Brunschwig, B. S.; Creutz, C.; Sutin, N. *Chem. Soc. Rev.* **2002**, *31*, 168.

(6) (a) Demadis, K. D.; Neyhart, G. A.; Kober, E. M.; Meyer, T. J. *J. Am. Chem. Soc.* **1998**, *120*, 7121. (b) Demadis, K. D.; El-Samanody, E.-S.; Coia, G. M.; Meyer, T. J. *J. Am. Chem. Soc.* **1999**, *121*, 535. (c) Lambert, C.; Noll, G. *J. Am. Chem. Soc.* **1999**, *121*, 8434. (d) Londergan, C. H.; Salsman, J. C.; Ronco, S.; Dolkas, L. M.; Kubiak, C. P. *J. Am. Chem. Soc.* **2002**, *124*, 6236. (e) Lear, B. J.; Glover, S. D.; Salsman, J. C.; Londergan, C. H.; Kubiak, C. P. *J. Am. Chem. Soc.* **2007**, *129*, 12772.

(7) Nelsen, S. F.; Konradsson, A. E.; Telo, J. P. *J. Am. Chem. Soc.* **2005**, *127*, 920.

(8) Nelsen, S. F.; Weaver, M. N.; Telo, J. P. *J. Am. Chem. Soc.* **2007**, *129*, 7036.

(9) Nelsen, S. F.; Konradsson, A. E.; Weaver, M. N.; Telo, J. P. *J. Am. Chem. Soc.* **2003**, *125*, 12493.

(10) Nelsen, S. F.; Weaver, M. N.; Zink, J. I.; Telo, J. P. *J. Am. Chem. Soc.* **2005**, *127*, 10611.

(11) Telo, J. P.; Grampp, G.; Shohoji, M. C. B. L. *Phys. Chem. Chem. Phys.* **1999**, *1*, 99.

(12) Bacon, R. G. R.; Lindsay, W. S. *J. Chem. Soc.* **1958**, 1375.

(13) Heller, E. J. *Acc. Chem. Res.* **1981**, *14*, 368.

(14) Nelsen, S. F.; Newton, M. D. *J. Phys. Chem. A* **2000**, *104*, 10023.

(15) Klamt, A.; Schüürmann, G. *J. Chem. Soc., Perkin Trans. 2* **1993**, 799.

(16) Clark, T.; Alex, A.; Beck, B.; Burkhardt, F.; Chandrasekhar, J.; Gedeck, P.; Horn, A. H. C.; Hutter, M.; Martin, B.; Rauhut, G.; Sauer, W.; Schindler, T.; Steinke, T. VAMP 9.0; Erlangen, 2003.

(17) Nelsen, S. F.; Weaver, M. N.; Konradsson, A. E.; Telo, J. P.; Clark, T. *J. Am. Chem. Soc.* **2004**, *126*, 15431.

(18) Nelsen, S. F.; Weaver, M. N.; Bally, T.; Yamazaki, D.; Komatsu, K.; Rathore, R. *J. Phys. Chem. A* **2007**, *111*, 1667.

(19) Nelsen, S. F.; Tran, H. Q. *J. Phys. Chem. A* **1999**, *103*, 8139.

(20) Creutz, C. *Prog. Inorg. Chem.* **1983**, *30*, 1.

(21) Joachim, A. C.; Launay, J. P.; Woitellier, S. *Chem. Phys.* **1990**, *147*, 131.

(22) Broo, A.; Larsson, S. *Chem. Phys.* **1990**, *148*, 103.

(23) Paddon-Row, M. N.; Wong, S. S. *Chem. Phys. Lett.* **1990**, *167*, 432.

(24) Ratner, M. A. *J. Phys. Chem.* **1990**, *94*, 4877.

(25) Nelsen, S. F.; Weaver, M. N.; Luo, Y.; Lockard, J. V.; Zink, J. I. *Chem. Phys.* **2006**, *324*, 195.

(26) Nelsen, S. F.; Luo, Y.; Weaver, M. N.; Lockard, J. V.; Zink, J. I. *J. Org. Chem.* **2006**, *71*, 4286.

(27) Valverde-Aguilar, G.; Wang, X.; Plummer, E.; Lockard, J. V.; Zink, J. I.; Nelsen, S. F.; Luo, Y.; Weaver, M. N. *J. Phys. Chem. A* **2008**, *112*, 7332.

(28) Although more than one type of charge-localized structure could clearly in principle be present, we have no evidence that ones with significantly different optical spectra would be present for the compounds under discussion, and we only consider two species here.

(29) (a) Gould, I. R.; Noukakis, D.; Gomez-Jahn, L.; Young, R. H.; Goodman, J. L.; Farid, S. *Chem. Phys.* **1993**, *176*, 439. (b) Gould, I. R.; Young, R. H.; Mueller, L. J.; Albrecht, A. C.; Farid, S. *J. Am. Chem. Soc.* **1994**, *116*, 8188; Appendix A3.

(30) Nelsen, S. F. *Chem.-Eur. J.* **2000**, *6*, 581.

JP807602K